CHEMISTRY OF MATERIALS
Communication

Chem. Mater. **2009,** *21,* 4753–4755 4753
DOI:10.1021/cm9024149

Lithium Ion Intercalation Performance of Niobium Oxides: KNb_5O_{13} and $K_6Nb_{10.8}O_{30}$

Jian-Tao Han, Dong-Qiang Liu, Sang-Hoon Song, Youngsik Kim, and John B. Goodenough*

Texas Materials Institute, ETC 9.102, University of Texas at Austin, Austin, Texas 78712

Received August 5, 2009
Revised Manuscript Received September 16, 2009

Carbonate-based electrolytes are presently used in rechargeable Li batteries. If the anode of such a battery has its Fermi energy less than 1 eV below the Fermi energy of elemental lithium, it reduces the electrolyte to form a passivating solid-electrolyte-interface (SEI) layer on which metallic lithium is deposited during a fast charge of the battery.[1−4] Dendrites tend to form on the lithium; the dendrites can grow to short-circuit the battery and ignite the electrolyte.[5] Therefore, safety concerns have led to a search for an anode material having a redox couple in the range 1.0−1.5 eV below the Fermi energy of lithium. Already reported[6−9] as a stable anode is $Li_4Ti_5O_{12}$ operating on the Ti^{4+}/Ti^{3+} redox couple located at 1.5 versus Li^+/Li. We have restricted our search to Li-insertion compounds because they have a smaller volume change over a charge/discharge cycle than do anodes operating on a displacement reaction. Here we report the position of the Nb^{5+}/Nb^{4+} couple in two oxide hosts, KNb_5O_{13} and $K_6Nb_{10.8}O_{30}$, that exhibit reversible Li insertion in the targeted voltage range.

KNb_5O_{13} is isostructural with KTa_5O_{13}, which was considered a "chemical twin" of α-PbO_2 by Awadalla and Gatehouse.[10] The KNb_5O_{13} framework contains *a*−*b* slabs of edge-sharing NbO_6 octahedra arranged to create periodic corner-sharing *c*-axis connections between neighboring slabs that give strong 3D bonding. The corner-sharing octahedra are separated by an octahedron sharing only edges, which creates intersecting perpendicular 1D tunnels parallel to the *a* and *b* axes in an *a*-*b* plane of the orthorhombic *Pbmc* (No. 57) structure with lattice parameters $a = 5.6720\,(20)$ Å, $b = 10.7370\,(50)$ Å, $c = 16.7420\,(60)$ Å.[11] Figure 1A shows the structure viewed along the *a* axis. Although K^+ ions occupy the tunnels, there is also room to insert Li^+ ions into them, which allows probing the energy of the Nb^{5+}/Nb^{4+} couple. Edge-sharing of NbO_6 octahedra allows Nb−Nb interactions within a slab that lower the bottom of the itinerant electron band of Nb^{5+}/Nb^{4+} redox states within a slab.

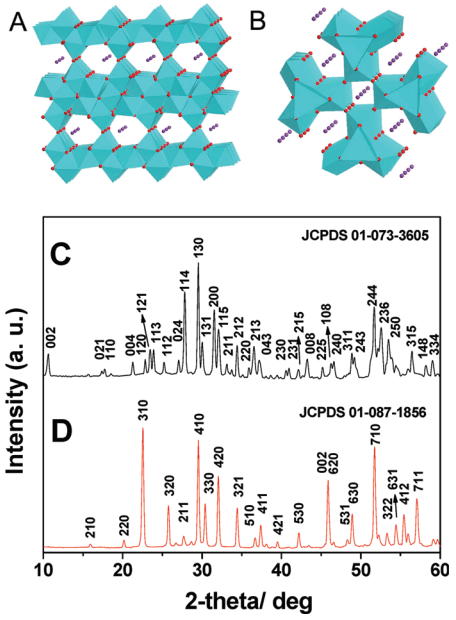

Figure 1. (A) Crystal structure view of KNb5O13 in b-c plane; (B) crystal structure view of $K_6Nb_{10.8}O_{30}$ in a-b plane; (C) XRD pattern of KNb_5O_{13}; (D) XRD pattern of $K_6Nb_{10.8}O_{30}$.

The structure of $K_6Nb_{10.8}O_{30}$ has a framework based on that of the tetragonal bronze structure of $K_{0.6}WO_3$ in which cooperative rotations about the *c*-axis of the corner-shared $WO_{6/2}$ octahedra create three types of *c*-axis tunnels: pentagonal, square, and triangular in cross-section.[12] Figure 1B shows the structure of $K_6Nb_{10.8}O_{30}$ viewed along the *c*-axis; the pentagonal and square tunnels parallel to the *c* axis are visible, the excess Nb^{5+} ions occupy the triangular tunnels to share edges with the octahedra.[13] Although the K^+ ions occupy both the pentagonal and square tunnels, it is nevertheless possible to insert Li^+ ions into the structure.

Polycrystalline KNb_5O_{13} and $K_6Nb_{10.8}O_{30}$ were prepared by conventional solid state reaction (SSR) (see the Supporting Information).[11,14] Figure 1C and D show the

*Corresponding author.

(1) Andersson, A. M.; Edstrom, K. *J. Electrochem. Soc.* **2001**, *148*, A1100.
(2) Peled, E.; Golodnitsky, D.; Ardel, G.; Eshkenazy, V. *Electrochim. Acta* **1995**, *40*, 2197.
(3) Ein-Eli, Y. *Electrochem. Solid-State Lett.* **1999**, *2*, 212.
(4) Wang, Y. F.; Guo, X. D.; Greenbaum, S.; Liu, J.; Amine, K. *Electrochem. Solid-State Lett.* **2001**, *4*, A68.
(5) Wu, M. S.; Chiang, P. J.; Lin, J. C.; Jan, Y. S. *Electrochim. Acta* **2004**, *49*, 1803.
(6) Thackeray, M. M. *J. Electrochem. Soc.* **1995**, *142*, 2558.
(7) Zaghib, K.; Simoneau, M.; Armand, M.; Gauthier, M. *J. Power Sources* **1999**, *81*, 300.
(8) Nakahara, K.; Nakajima, R.; Matsushima, T.; Majima, H. *J. Power Sources* **2003**, *117*, 131.
(9) Cheng, L.; Liu, H.-J.; Zhang, J.-J.; Xiong, H.-M.; Xia, Y.-Y. *J. Electrochem. Soc.* **2006**, *153*, A1472.
(10) Awadalla, A.-A.; Gatehouse, B.-M. *J. Solid-State Chem.* **1978**, *24*, 183.
(11) Kwak, J. E.; Yun, H.; Hee, K. C. *Acta Crystallogr., Sect. E* **2005**, *61*, i132.
(12) Wadsky, A. D., *Non-stoichiometric Compounds*; Mandelcorn, L., Ed. l Academic Press: New York, 1964; p 134.
(13) Beeker, P.; Held, P. *Z. Kristallogr.* **2000**, *215*, 319.
(14) Zhang, G.-K.; Hu, Y.-J.; Ding, X.-M.; Zhou, J.; Xie, J.-W. *J. Solid State Chem.* **2008**, *181*, 2133.

Published on Web 09/22/2009

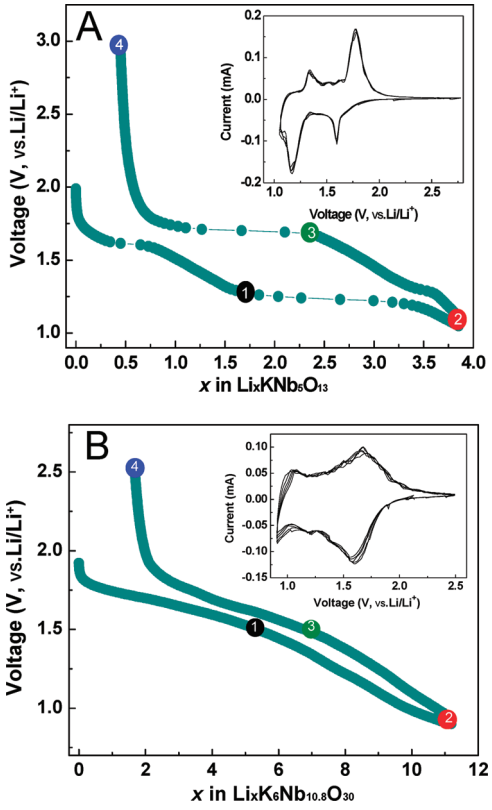

Figure 2. (A) Voltage−composition profiles of KNb_5O_{13} (obtained at 15 mA/g), the inset shows the CV curves at a scan rate of 0.05 mV/s; (B) Voltage−composition profiles of $K_6Nb_{10.8}O_{30}$ (obtained at 25 mA/g), the inset shows the CV curves at a scan rate of 0.05 mV/s. The Li content x is obtained from $xW/MF = I(A)t(s)$, where W and M are the weight and mole weight of active material, respectively, and F is the Faraday constant.

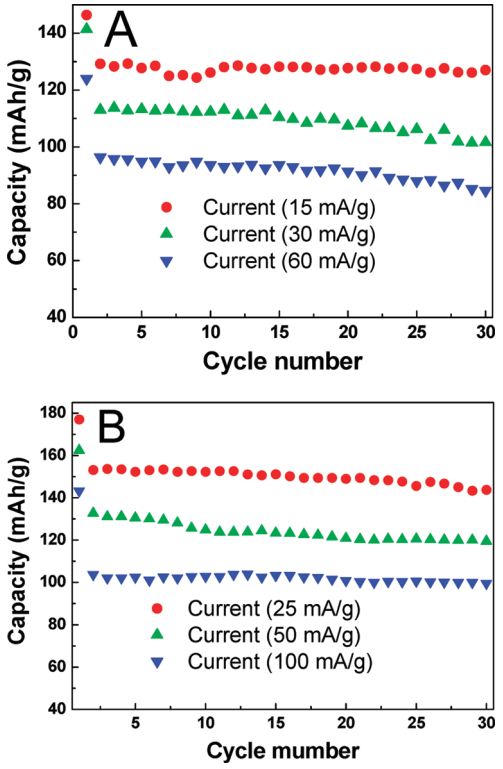

Figure 3. (A) Cycle−life performance of the KNb_5O_{13} operated between 1.0 and 3.0 V at rate of 15, 30, and 60 mA/g, respectively; (B) corresponding capacity−retention curves of the $K_6Nb_{10.8}O_{30}$ operated between 0.9 and 2.5 V at a rate of 25, 50, and 100 mA/g, respectively.

XRD patterns of KNb_5O_{13} and $K_6Nb_{10.8}O_{30}$. All the peaks in both the XRD patterns are indexed according to the JCPDS card no. 073−3605 and 87−1856, respectively. Phase-pure samples were obtained. The lattice parameters of KNb_5O_{13}, refined by the Rietveld method with the Fullprof program,[15] are a = 5.6789 Å, b = 10.7547 Å, and c = 16.7230 Å. The lattice parameters of $K_6Nb_{10.8}O_{30}$ are a = 12.4777 Å and c = 3.9529 Å (Figures S1 and S2 in the Supporting Information). The morphology and microstructure of the samples were investigated with scanning electron microscopy (Figure S3 and S4, respectively, in the Supporting Information).

The electrochemical performances of the materials were tested versus lithium with 20% w/w carbon black. Panels A and B in Figure 2 show voltage−composition traces for KNb_5O_{13}/Li and $K_6Nb_{10.8}O_{30}$/Li cells cycled by passing a constant current of 15 and 25 mA/g, respectively (the insets show the CV curves). The KNb_5O_{13}/Li cell shows two voltage plateaus located near 1.6 and 1.2 V with a stable reversible capacity of 130 mAh/g. The $K_6Nb_{10.8}O_{30}$/Li cell shows a solid-solution range for 0.9 V < V < 1.7 V with a reversible capacity of about 160 mA h/g and an overall uptake capacity of 11.2 Li per formula unit. Figures 3A and B illustrate specific capacity vs cycle number on being discharged and charged at different rates for a total of 30 cycles for the samples of KNb_5O_{13} and $K_6Nb_{10.8}O_{30}$. The stable reversible capacities are around 90 and 110 mA h/g at the current densities of 60 and 100 mA/g, respectively (Figures S5 and S6 in the Supporting Information).

The two plateaus in Figure 2A represent two-phase regions, but their compositional ranges are shifted on charge relative to discharge, which gives an unusual polarization hysteresis associated with a first-order phase change. This unusual phenomenon is reproducible on repeated charge/discharge cycles.

To gain further insight into the insertion mechanisms, ex situ XRD analyses were performed at selected voltage points 1−4 (Figures 2 A and B). Variations of peak position, shape, and relative intensity were not distinguishable. No additional peaks were observed after 30 cycles, indicating that no new phases were formed during the first 30 cycles (Figure 4 A and C). However, as shown in Figure 4 B, the [114] peaks of KNb_5O_{13} shifted continuously toward lower angles during the insertion of Li and then shifted back on removal of Li, which was confirmed by the crystal dimensional variations in the process of Li insertion/extraction (Table S1 and S2 in the Supporting Information).

The XRD patterns show that the framework structure changes little, so we postulate that the two-phase regions reflect Li^+ ion orderings in the tunnels and that ordered regions form first at the entrance of the tunnels and grow down the tunnels on discharge, but they are disordered

(15) Carvajal, J.-R. FULLPROF Version 2K; Laboratoire Leon Brillouin CEA−CNRS: Saclay, France, **2000**.

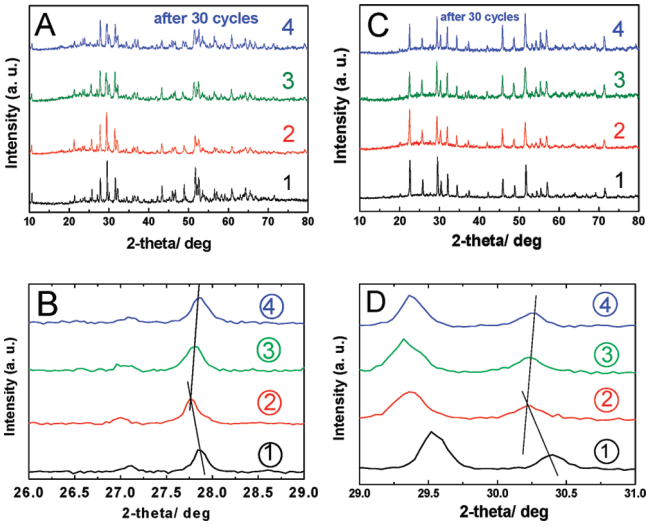

Figure 4. (A, B) XRD patterns of the KNb_5O_{13}; (C, D) XRD patterns of the $K_6Nb_{10.8}O_{30}$.

first at the entrance on charge to give the polarization hysteresis. The fact that the small shift of the [114] peaks is reversible indicates that there is little exchange of K^+ and Li^+ ions in a discharge/charge cycle. As a further check on this latter inference, we tried to ion exchange Li^+ for K^+ chemically; these attempts resulted in a decomposition of the framework.

The large overlap of 4d orbitals on Nb ions sharing common octahedral-site edges gives an itinerant electron band of Nb t orbital parentage that stabilizes the bottom of the band and therefore the electrons of a formal Nb^{5+}/Nb^{4+} couple. Corner-shared octahedra have a Nb−Nb 4d orbital overlap that depends on the extent of covalent mixing into the 4d orbitals of the $2p_\pi$ orbitals of the bridging oxygen; this overlap is probably weaker although also strong enough to give itinerant electrons in a narrow π^* band of t orbital parentage. Therefore, the bottom of the π^* band is expected to be at a higher energy than the t orbital band for edge-shared octahedra. Niobates with only corner-shared octahedra may offer lower voltages versus Li^+/Li.

In summary, the potassium-niobate family having tunnels occupied by K^+ ions offer reversible insertion of Li at acceptable capacities with voltages within the targeted voltage range of 1.0−1.5 V versus Li^+/Li. These frameworks contain Nb(V) in octahedral sites sharing edges. Where $Nb(V)O_6$ octahedra share only corners, we can expect the cell voltage versus Li^+/Li of to be lower than 1.5 V; if it falls below 1.0 V versus Li^+/Li, it would be plagued by formation of a thick SEI layer. The data for KNb_5O_{13} and $K_6Nb_{10.8}O_{30}$ that we report show that the Nb(V)/Nb(IV) couple in an oxide with only corner-shared NbO_6 octahedra could be of potential interest for the anode of a lithium ion battery having thermodynamic stability in the presence of a carbonate electrolyte. An inability to retain the Nb_5O_{13} and $Nb_{10.8}O_{30}$ frameworks on substitution of Li^+ for K^+ ions has prevented us from exploring further reduction of the framework of the Nb(IV)/Nb(III) couple. Nevertheless, improvement in reversible capacity should be possible with smaller particles; crystallite size has a strong influence on reversible capacity, as has been demonstrated, for example, with nanocrystalline $AlNbO_4$[16] and TiO_2.[17]

Acknowledgment. This work was supported by the office of FreedomCAR and Vehicle Technologies of the U.S. Department of Energy under Contract DE-AC03-76SF00098 and the Robert A. Welch Foundation, Houston, TX, Grant F-1066.

Supporting Information Available: Materials synthesis, electrode fabrication, and the lattice parameters based on the Rietveld refinement of the X-ray powder diffraction data of KNb_5O_{13} and $K_6Nb_{10.8}O_{30}$ (PDF). This material is available free of charge via the Internet at http://pubs.acs.org.

(16) Anji Reddy, M.; Varadaraju, U. V. *Chem. Mater.* **2008**, *20*, 4557.
(17) Armstrong, A. R.; Armstrong, G.; Canales, J.; Garcia, R.; Bruce, P. G. *Adv. Mater.* **2005**, *17*, 862.